

2008

Optimal In-Situ Bioremediation System Design Using Simulated Annealing

H. J. Shieh

R. C. Peralta

Utah State University

Follow this and additional works at: http://digitalcommons.usu.edu/cee_facpub

 Part of the [Civil and Environmental Engineering Commons](#)

Recommended Citation

Shieh, H. J. and R. Peralta. August 2008. Optimal In-Situ Bioremediation System Design Using Simulated Annealing. Transactions of the ASABE 51(4): 1-13.

This Article is brought to you for free and open access by the Civil and Environmental Engineering at DigitalCommons@USU. It has been accepted for inclusion in CEE Faculty Publications by an authorized administrator of DigitalCommons@USU. For more information, please contact dylan.burns@usu.edu.



OPTIMAL IN-SITU BIORMEDIATION SYSTEM DESIGN USING SIMULATED ANNEALING

H.-J. Shieh, R. C. Peralta

ABSTRACT. *The presented procedure combines continuous simulated annealing (CSA) heuristic optimization with BIOPLUME II simulation for optimizing in-situ bioremediation system design. The design goal is to minimize the total cost of facility installation and operation needed to achieve contaminant plume containment and cleanup. System design elements include pumping rates and well locations. During optimization, pumping rates are treated as continuous variables, differing from previously reported simulated annealing combinatorial optimization for groundwater management. To improve computation efficiency, CSA annealing schedules employing four different temperature update functions (TUF) are contrasted. Each yields somewhat different optimal designs and requires different computation effort. An adaptive TUF used almost 4,000 simulations to develop the lowest-cost design. A geometric TUF used 5% fewer simulations to create a design costing about 3% more. Site characteristics significantly affect optimal system design features. For a specific design, bioremediation improves with increasing hydraulic conductivity, longitudinal dispersivity, and remediation period and with decreasing retardation factor.*

Keywords. *Aerobic biodegradation, Continuous simulated annealing, Groundwater remediation, In-situ bioremediation, Optimization.*

In-situ bioremediation of contaminated groundwater is employed because of its cost-effective ability to achieve satisfactory cleanup. Major advantages can include lower capital cost and permanent contaminant elimination (Cookson, 1995). An in-situ bioremediation system consists of subsurface water delivery systems (injection wells or trenches) and extraction wells. The recharge water provides nutrients and terminal electron acceptors to stimulate microbial growth. The microorganisms transform contaminants to less harmful chemicals or mineral end products, such as carbon dioxide and water. Oxygen is the most common in-situ bioremediation electron acceptor. Downgradient wells extract contaminated groundwater to contain the plume and to enhance movement of electron acceptors and nutrients. Contaminated groundwater from the extraction wells is treated by air stripping or activated carbon. Downgradient monitoring wells are used to verify plume containment.

Desired is a cost-effective remediation system for removing sufficient contaminants to meet regulator requirements. In designing a system, modelers commonly use simulation models to predict remediation effectiveness and the cost of alternative system designs. Because of the

countless number of feasible designs, a trial-and-error simulation approach might never identify a truly optimal remediation system design. Design can be enhanced by combining simulation models with optimization techniques.

Coupled groundwater simulation model and optimization techniques have been reported for hydraulically managing groundwater, with or without surface waters, and for capturing contaminated groundwater. A simulation/optimization (S/O) management model directly incorporates a physical system simulation model with or within an optimization program that identifies the best management strategy. Such an optimal strategy maximizes (or minimizes) management objectives while satisfying constraints on hydraulics (pumping rates, hydraulic heads, hydraulic gradient, or velocities), concentration (maximum contaminant levels), and other variables.

S/O models that primarily optimize flows and heads usually employ traditional optimization methods, such as linear programming, nonlinear programming, dynamic programming, quadratic programming, and mixed-integer programming. However, some researchers have also addressed contaminant transport via traditional optimizers. For example, Cooper et al. (1998) optimized light nonaqueous phase liquid recovery using nonlinear programming.

S/O models explicitly addressing contaminant concentrations have been presented for remediation efforts, such as pump-and-treat operation, soil vapor extraction (Sun et al., 1996), and in-situ bioremediation (Minsker and Shoemaker, 1996). Minsker and Shoemaker (1998) coupled their successive approximation linear quadratic regulator (SALQR) with the Bio2D finite element biodegradation simulator. Their cost function considered pumping operation, maintenance, oxygen addition, and treatment costs. It did not include well installation and facilities capital costs.

Submitted for review in May 2007 as manuscript number SW 7035; approved for publication by the Soil & Water Division of ASABE in June 2008.

The authors are **Horng-Jer Shieh**, Assistant Professor, Department of Construction Technology and Spatial Information, Diwan University, Taiwan; and **Richard C. Peralta**, ASABE Member Engineer, Professor, Department of Biological and Irrigation Engineering, Utah State University, Logan, Utah. **Corresponding author:** Horng-Jer Shieh, Department of Construction Technology and Spatial Information, Diwan University, 87-1, Nansh Li, Madou, Tainan, Taiwan; phone: 886-6-571888; fax: 886-6-5718464; e-mail: hjshieh@dwu.edu.tw.

S/O models that incorporate contaminant transport simulators and constrain concentrations are termed transport optimizers. Most transport optimizers employ heuristic optimization (HO) techniques, such as simulated annealing (Dougherty and Marryott, 1991; Kuo et al., 1992; Marryott et al., 1993; Marryott, 1996; Rizzo and Dougherty, 1996; Wang and Zheng, 1998), genetic algorithm (McKinney and Lin, 1994; Aly and Peralta, 1999; Reed et al., 2000; Smalley et al., 2000; Gopalakrishnan et al., 2003; Chan-Hilton and Culver, 2005), and hybrid algorithms that might or might not include neural networks (Rogers and Dowl, 1994; Espinoza et al., 2005). HO methods are advantageous because they do not need to compute derivatives with respect to decision variables. Derivatives are sometimes difficult to estimate analytically or numerically in highly nonlinear and non-convex groundwater remediation problems.

Yoon and Shoemaker (1999) contrasted eight optimization methods for minimizing pumping costs for in-situ bioremediation of contaminated groundwater. These included variants of GA, direct search, and derivative-based techniques. The de-randomized evolutionary algorithm performed best. Smalley et al. (2000) used a noisy GA to minimize in-situ bioremediation cost (including monitoring cost, remediation well capital and operating costs). Yoon and Shoemaker (2001) used both binary-coded GA and real-coded GA with directive recombination and screened replacement for minimizing total pumping cost of in-situ groundwater bioremediation system.

A desirable attribute of simulated annealing (SA) optimizers (Corana et al., 1987) is that convergence to a globally optimal solution has been proven for the functions minimization of continuous variables. For dewatering, Dougherty and Marryott (1991) assumed five wells and six discrete pumping rates (solution space of $6^5 = 7776$ possible states) and used SA to minimize the pumping plus well installation cost. Rizzo and Dougherty (1996) applied SA to determine time-varying remediation well locations that minimize construction, operation, and maintenance costs of achieving volatile organic chemical cleanup within 30 years. In these SA applications, the decision variables are restricted to discrete values such as a specified number of pumping rates and well locations (Dougherty and Marryott, 1991; Rizzo and Dougherty, 1996). Wang and Zheng (1998) compared nonlinear programming, GA, and SA to maximize extracted groundwater while minimizing pumping cost. Well cost versus capacity was assumed to be a continuous function and hence suitable for nonlinear programming. Pumping decision variables were treated as discrete values both in SA and GA. The precision of decision variables depends on the number of decimal points used for the generated random number. The SA performed significantly better than the GA for the maximum yield water supply problem.

By contrast with previous work, we here: (1) extend SA application to treat pumping rates as continuous decision variables and use Corana's neighborhood function, (2) compare four SA algorithms with different annealing schedules for optimal in-situ bioremediation system design, and (3) design an in-situ bioremediation system that minimizes total system installation plus operation cost. Continuous simulated annealing (CSA) can address such a stepwise system cost function for which derivatives are difficult to estimate analytically or numerically. Decision variables include pumping well locations and pumping

(extraction and injection) rates. The designed system must satisfy constraints on pumping rates, hydraulic heads, and contaminant concentration at the plume source and at downstream monitoring wells. Subsequent discussion contrasts the effect of CSA annealing schedule (AS) parameter set selection on optimal solution qualities and required computational time and discusses optimal system design sensitivity to site and contaminant properties.

IN-SITU BIOREMEDIATION OPTIMIZATION PROBLEM FORMULATION

Here, the objective function is to minimize total cost of extraction and injection well installation, facility capital costs, and operation costs. This is more realistic for new system designs than an objective function that includes only operation cost (Ren and Minsker, 2005). Historically, most groundwater optimization research has involved optimizing operation only (Culver and Shoemaker, 1997; Johnson and Rogers, 2000). However, capital facility installation costs can be significant, especially when optimizing for short (such as five year) groundwater remediation efforts, (Culver and Shoemaker, 1997; Kalwij and Peralta, 2006). The desirability of optimizing capital costs and operation costs together is recognized (Peralta et al., 2008).

$$\text{Minimize } Z = \sum_{e=1}^{M^P} C^P(e)p(e) + \sum_{e=1}^{M^P} C^{IP}(e)IP(e) + D \left(\sum_{e=1}^{M^i} p(e) \right) + E \left(\sum_{e=1}^{M^e} p(e) \right) \quad (1)$$

where

- Z = total cost of in-situ bioremediation system
- e = index denoting a candidate injection or extraction location
- p(e) = injection or extraction rate at location e (L^3/T)
- $C^P(e)$ = cost coefficient for injection (including oxygen, nutrient, and pumping costs) or extraction (including treatment and pumping operation costs) (\$ per L^3/T)
- M^P = total number of injection and extraction wells
- $C^{IP}(e)$ = injection or extraction well installation cost at location e (\$ per well)
- IP(e) = zero-one integer for injection or extraction well existence at location e
- $D \left(\sum_{e=1}^{M^i} p(e) \right)$ = oxygen and nutrient injection facility capital cost, a function of total injection rate (\$)
- M^i = total number of injection wells
- $E \left(\sum_{e=1}^{M^e} p(e) \right)$ = treatment facility capital cost, a function of total extraction rate (\$)

M^e = total number of extraction wells
 M^P = $M^i + M^e$.

The stepwise functions of injection and treatment facilities capital costs are discontinuous because of specific sizes of pipes, pumps, and facilities. Capital cost of injection facility D can be expressed as:

$$D \left(\sum_{e=1}^{M^i} p(e) \right) = 0 \quad \text{if} \quad \sum_{e=1}^{M^i} p(e) = 0$$

$$= D_q \quad \text{if} \quad CD_{q-1} < \sum_{e=1}^{M^i} p(e) \leq CD_q$$

$$q = 1, 2, \dots, M^Q \quad (2)$$

where D_q is the capital cost of the injection facility when total injection rate is between design injection capacity CD_{q-1} and CD_q , and M^Q is the total number of alternative design injection capacities. Injection capacity CD_0 equals 0. Equation 3, defining treatment facility E capital cost, is analogous to equation 2 and obtained by substituting:

$$E \left(\sum_{e=1}^{M^e} p(e) \right) \quad \text{for} \quad D \left(\sum_{e=1}^{M^i} p(e) \right), \quad M^e \text{ for } M^i, \quad E_q \text{ for } D_q, \quad CE_q$$

for CD_q , and M^R for M^Q , where E_q is the treatment facility capital cost when total extraction rate is between design treatment capacity CE_{q-1} and CE_q , and M^R is the total number of alternative design treatment capacities. Treatment capacity CE_0 is 0. The equation of treatment facility E capital cost is expressed as:

$$E \left(\sum_{e=1}^{M^e} p(e) \right) = 0 \quad \text{if} \quad \sum_{e=1}^{M^e} p(e) = 0$$

$$= E_q \quad \text{if} \quad CE_{q-1} < \sum_{e=1}^{M^e} p(e) \leq CE_q$$

$$q = 1, 2, \dots, M^R \quad (3)$$

Management model constraints include the following:

- Upper and lower bounds on injection and extraction rates.
- Bounds on aquifer hydraulic head at injection and extraction wells.
- Upper bound on final contaminant concentration to achieve a cleanup standard:

$$C_{k,Te} \leq C_{cl} \quad \forall k \in \Psi \quad (4)$$

where $C_{k,Te}$ is the contaminant concentration at node k in the end of remediation time Te (M/L^3), C_{cl} is the contaminant concentration of cleanup standard (M/L^3), and Ψ is a set of locations where cleanup standard concentration are enforced. In this study, Ψ includes all study area nodes.

- Upper bound on concentration at specific locations to assure plume containment (prevent unacceptable concentration migration):

$$C_{o,Te} \leq C_{ca} \quad \forall o \in \Omega \quad (5)$$

where $C_{o,Te}$ is the allowable contaminant concentration at node o in the end of remediation time Te (M/L^3), C_{ca} is the allowable contaminant concentration (M/L^3), and Ω is a set of monitoring wells.

SIMULATED ANNEALING

INTRODUCTION TO SIMULATED ANNEALING

Simulated annealing is an algorithmic approach for combinatorial optimization problems (Kirkpatrick et al., 1983; van Laarhoven and Aarts, 1987; Aarts and Korst, 1989; Otten and van Ginneken, 1989). SA is also known as statistical cooling (Aarts and van Laarhoven, 1985), probabilistic hill climbing (Romeo and Sangiovanni-Vincentelli, 1985), and stochastic relaxation (Geman and Geman, 1984). SA uses "hill climbing" moves under a certain probability distribution (Cerny, 1985; Kirkpatrick et al., 1983) to escape from a local optimum and obtain a globally optimal solution. SA convergence to globally optimal solutions has been proven using homogeneous and inhomogeneous Markov chain theory (Geman and Geman, 1984; Hajek, 1988; Romeo and Sangiovanni-Vincentelli, 1991).

Key SA algorithm elements (fig. 1) include: (1) neighborhood function, (2) accepting function, (3) annealing schedule, and (4) cost function. Cost function depends upon optimization problem objectives. The other three elements control the efficiency and quality of optimal solutions. The neighborhood function generates the new system configuration based on random movements. An annealing schedule includes initial temperature, temperature update function (TUF), inner-loop criterion, and outer-loop criterion. We specify the initial temperature such that 80% to 90% of new configurations will be accepted by the accepting function. The temperature update function controls temperature decrement. It reduces the temperature slowly to ensure convergence to optimality in the continuous solution space. For each selected temperature, a number of optimal solutions are evaluated in the inner-loop procedure. For the SA algorithm to reach equilibrium at a fixed temperature, a number of inner-loop movements are necessary. The outer loop terminates when the stopping criterion is satisfied, recognizing that the algorithm has reached a good optimal solution and further temperature decrease cannot improve the solution. Below is a detailed discussion of these elements based on theoretical results and numerical experiments.

NEIGHBORHOOD FUNCTION

The major difference between continuous simulated annealing and discrete simulated annealing (DSA) is the configuration space of decision variables. In the combinatorial optimization problem, the configuration space is discrete. The number of system configurations is fixed. In CSA, the number of states in the configuration space is not fixed. This makes searching for the optimal solution in continuous space more difficult than in discrete space. The neighborhood function, which randomly produces new configurations derived from an initial configuration, affects the efficiency of the search for optimal solutions in continuous space.

Many researchers have proposed different neighborhood functions for CSA (Vanderbilt and Louie, 1984; Bo-

```

initialize T, X, C; /* T = temperature, X = optimal solutions, C = cost */

while (stopping criterion is not satisfied)

{ while (inner-loop criterion is not satisfied)

    { Cnew = cost function(Xnew);

      ΔC = Cnew - Cold;

      if ( accepting function(ΔC, T) )

          accept Xnew new optimal solutions;

      else

          reject Xnew new optimal solutions; }

    update temperature T; }

```

Figure 1. Pseudo code of continuous simulated annealing algorithm.

hachevsky et al., 1986; Corana et al., 1987; Dekkers and Aarts, 1991; Wang and Chen, 1996). Applying such functions to many test problems and numerical experiments has shown their ability to obtain global optimal solutions. In this article, we employ a neighborhood function approach proposed by Corana et al. (1987). The step size of this neighborhood function varies with the SA algorithm accepting ratio. The intent is to maintain a 0.5 accepting ratio (half of the new configurations are accepted and half are rejected at any temperature). These procedures are:

Step 1. Specify initial point X_i or select it randomly from the configuration space.

Step 2. Generate a random number r_n from the uniform distribution in the range $[-1, 1]$.

Step 3. $X_i' = X_i + r_n w_i^{n+1}$:

$$w_i^{n+1} = w_i^n [1 + C_u (R_a - 0.6) / 0.4] \text{ if accepting ratio } R_a > 0.6,$$

$$w_i^{n+1} = w_i^n \text{ if accepting ratio } 0.4 < R_a < 0.6,$$

$$w_i^{n+1} = w_i^n / [1 + C_u (0.4 - R_a) / 0.4] \text{ if accepting ratio } R_a < 0.4,$$

where n is the temperature step, w_i^0 is the initial step size, and C_u is the parameter controlling the step size variation.

ACCEPTING FUNCTION

The Metropolis algorithm is a well-known stochastic accepting function (Metropolis et al., 1953). An alternative to the Metropolis algorithm is a threshold accepting function that reduces SA computational cost or avoids using random numbers and exponential functions (Dueck and Scheuer, 1990; Moscato and Fontanari, 1990; Stiles, 1994; Lin et al., 1995). Althofer and Koschnick (1991) presented convergence results for a SA threshold accepting function. A threshold accepting function accepts or rejects a new configuration based on T . If $\Delta C > 0$ (indicating the new configuration does not reduce the cost), the new configuration can still be accepted if $\Delta C < T$. This allows an uphill move to escape a local optimum. However, decreasing

temperature makes it more difficult to accept a new configuration that increases cost. Here we employ a threshold accepting function. It uses a deterministic rule to accept or reject a new configuration. Advantages are a reduction in number of simulations and a screening-out of expensive system designs.

ANNEALING SCHEDULES

An annealing schedule is a key SA element, and includes (1) initial temperature, (2) temperature update function (TUF), (3) inner-loop criterion (finite length of Markov chain), and (4) outer-loop criterion. Annealing schedules control algorithm convergence toward optimal solutions. Annealing schedules can be classified as either static schedules or adaptive schedules (Kirkpatrick et al., 1983; Aarts and van Laarhoven, 1985; Romeo and Sangiovanni-Vincentelli, 1985; Huang et al., 1986; Szu and Hartley, 1987; Ingber, 1989). A static schedule has parameters fixed before the algorithm is started. An adaptive schedule uses a feedback control to change parameters during algorithm operation. The temperature decrement is adjusted by measuring the rate of change of the objective function or the rate at which the solution space is being searched. Annealing schedule selection helps speed SA convergence and reduces computational cost. Romeo and Sangiovanni-Vincentelli (1991) concluded that static and adaptive schedules efficiency can only be determined experimentally.

Initial Temperature

The initial temperature must be high enough to guarantee a high accepting probability for the solution space search. In a static annealing schedule, the initial temperature should be specified such that 80% to 90% of new configurations will be accepted by the accepting function. The initial temperature is related to the optimization problem cost function, the neighborhood function, and the accepting function. Determining a suitable initial temperature is a trial-and-error effort.

Temperature Update Function

Here we consider four temperature update functions (TUFs) for CSA application. The following two TUFs are classified as static annealing schedules. First is a geometric temperature update function expressed as:

$$T_{n+1} = \alpha T_n \quad (6)$$

where α is the parameter controlling rate of temperature cooling. The range of α is between 0.80 and 0.99. Second is the fast SA TUF:

$$T_{n+1} = \frac{T_0}{1+n} \quad (7)$$

The temperature update is inversely linear to a function of time n given a sufficiently high initial temperature T_0 .

In an adaptive annealing schedule, the rate of decreasing temperature is neither fixed nor linear (as is the TUF in a static annealing schedule). Aarts and van Laarhoven (1985) presented the first of the two adaptive TUFs we apply. When implemented into a CSA, the adaptive TUFs successfully obtained the global minimum of several test functions (Dekkers and Aarts, 1991). This TUF is expressed as:

$$T_{n+1} = \frac{T_n}{1 + \left[T_n \frac{\ln(1 + \delta)}{3\sigma_c} \right]} \quad (8)$$

where σ_c represents the standard deviation of cost at temperature T_n , and the constant δ denotes the distance parameter, which determines the speed of temperature decrement. The second adaptive TUF is expressed by Huang et al. (1986) as:

$$T_{n+1} = T_n \cdot \exp\left(-\frac{\lambda T_n}{\sigma_c}\right) \quad (9)$$

where λ is the control parameter of temperature decrement ($\lambda \leq 1$). In the application of equation 9, the decreasing rate of T_{n+1}/T_n is lower bounded by 0.5 to prevent premature convergence. Dougherty and Marrayott (1991) applied this TUF to optimize groundwater management.

Inner-Loop Criterion

The CSA algorithm is described by a sequence of homogeneous Markov chains. Each Markov chain is generated at a fixed temperature. The length of a Markov chain is equivalent to the number of movements performed by the neighborhood function in the CSA inner-loop. The theoretical proof of the CSA algorithm states that an infinite length Markov chain is a necessary condition for reaching a stationary probability distribution. This means that an infinite number of movements in the inner loop is a necessary condition for the CSA algorithm to reach equilibrium at a fixed temperature. As T approaches 0 (via temperature update function), the optimal solution generated by the algorithm converges to a global optimum. In practical application, one should use a fixed length of Markov chain that is sufficiently large for a continuous SA algorithm to explore the solution space. Basing this length on the size of optimization problem yields:

$$L = L_0 m \quad (10)$$

where L_0 is a constant called the standard length, and m is the number of decision variables. Dekkers and Aarts (1991) recommended $L_0 = 10$ for finding the global minimum of several test functions via CSA algorithm. Marrayott et al. (1993) determined that standard length L_0 should be between 10 and 100 for groundwater remediation problems.

Outer-Loop Criterion

The final annealing schedule component is the outer-loop criterion, also called a stopping criterion. The stopping criterion is used to recognize that the algorithm has reached a good optimal solution and further temperature decrease cannot improve the optimal solution (Kirkpatrick et al., 1983; Aarts and van Laarhoven, 1985; Huang et al., 1986). Commonly, when average cost does not change significantly for several successive temperature decrements, the algorithm stops and the system is considered "frozen" at the optimal solution (Kirkpatrick et al., 1983). In this study, two stopping criteria are employed. The first stopping criterion is a pre-specified final temperature. The CSA algorithm terminates when T reaches or passes the final temperature. This avoids an infinite loop of CSA runs. The second stopping criterion terminates CSA runs when the average cost does not change after ten successive temperature decrements.

CONSTRAINTS HANDLING

There are two methods for handling constraints in SA applications. The first, a death penalty heuristic, involves restricting the solution space to solutions that conform to the constraints. If a system design does not satisfy all the constraints, it is automatically rejected. The second employs a suitably defined penalty function for the constraints. The penalty cost will be added to the total cost for the violated constraints. For constrained engineering problems, the penalty function method is more flexible than a death penalty heuristic. Moreover, the system design can reach the optimal solution easier if the search is allowed to cross an infeasible region. Bennage and Dhingra (1995) concluded that a penalty function incorporating design constraints yielded the best results for structural engineering optimization.

Here we deal with the inequality constraints by expanding the objective function to include penalty cost for infeasible solutions. A penalty cost function is defined as:

$$f_j(X) = \begin{cases} Pe(j)g_j(X) & \text{for violated constraint } g_j(X) > 0 \\ 0 & \text{for satisfied constraint } g_j(X) \leq 0 \end{cases} \quad (11)$$

where $f_j(X)$ is a penalty cost function for the j th constraint ($g_j(X) \leq 0$), and $Pe(j)$ is a penalty coefficient for the j th constraint. The penalty cost is calculated by the distance from feasibility multiplied by a penalty cost coefficient for the violated constraint (i.e., if $g_j(X) > 0$). If the constraint is satisfied (i.e., if $g_j(X) \leq 0$), the penalty cost is zero. Specifying penalty coefficients is challenging. A high penalty coefficient will keep most of the search in the feasible solution space but can lead to a costly conservative system design. A low penalty coefficient permits searching both feasible and infeasible regions, but can cause convergence to an infeasible system design. Here we apply a dynamic penalty function, a technique used to solve nonlinear constrained optimization problems with genetic algorithms (Joines and Houck, 1994; Michalewicz and Attia, 1994). Penalty coefficients are not fixed, but increase as T decreases. Initially penalty coefficients are small to promote searching both feasible and infeasible regions. As T decreases, penalty coefficients increase, encouraging the CSA to find a feasible solution.

$$Pe_{n+1} = \frac{Pe_0}{T_{n+1}} \quad (12)$$

where Pe_{n+1} is the penalty coefficient at temperature step $n+1$, and Pe_0 is the initial penalty coefficient.

BIODEGRADATION MODELING

Several computer models incorporate microbial growth and biodegradable pollutant transport in groundwater. These are generally based upon a macroscopic conceptual model that does not assume a particular microorganism distribution within the pore space. Organic contaminant removal occurs by Monod or Michaelis-Menten kinetics involving aerobic degradation and anaerobic degradation (Borden and Bedient, 1986; MacQuarrie et al., 1990; Malone et al., 1993; Essaid et al., 1995). The BIOPLUME II simulation model employs the macroscopic concept and assumes that aerobic biodegradation is instantaneous (Rifai et al., 1988; Rifai and Bedient, 1990). It uses oxygen as the electron acceptor.

BIOPLUME II uses a dual-particle mover procedure to simulate subsurface oxygen and contaminant transport. It was developed by modifying a two-dimensional method of characteristics (MOC) transport model (Konikow and Bredehoeft, 1978). The contaminant and oxygen transport equations are solved at every time step to calculate contaminant and oxygen distributions (Rifai et al., 1988):

$$\frac{\partial(Cb)}{\partial t} = \frac{1}{R_c} \left[\frac{\partial}{\partial x_i} \left(bD_{ij} \frac{\partial C}{\partial x_j} \right) - \frac{\partial}{\partial x_i} (bCV_i) \right] - \frac{C'W}{n_e} \quad (13)$$

$$\frac{\partial(Ob)}{\partial t} = \left[\frac{\partial}{\partial x_i} \left(bD_{ij} \frac{\partial O}{\partial x_j} \right) - \frac{\partial}{\partial x_i} (bOV_i) \right] - \frac{O'W}{n_e} \quad (14)$$

where C and O are contaminant and oxygen concentrations (M/L^3), respectively; C' and O' are contaminant and oxygen concentrations in a source or sink fluid (M/L^3); n_e is the effective porosity; b is the aquifer saturated thickness (L); t is time (T); x_i and y_j are Cartesian coordinates (L); W is the volume flux per unit area (L/T); V_i is the seepage velocity in the direction of x_i (L/T); R_c is the retardation factor for contaminant; and D_{ij} is the hydrodynamic dispersion coefficient (L^2/T).

Contaminant and oxygen plumes are combined using superposition to simulate instantaneous reaction between oxygen and contaminants. Essaid et al. (1995) confirmed the findings of Rifai and Bedient (1990) that aerobic degradation can be treated as occurring instantaneously. Contaminant and oxygen concentration decreases are calculated from:

$$\Delta C_{RC} = O/F; O = 0 \text{ where } C > O/F \quad (15)$$

$$\Delta C_{RO} = CF; C = 0 \text{ where } O > CF \quad (16)$$

where ΔC_{RC} and ΔC_{RO} are the calculated change in contaminant and oxygen concentrations, respectively; and F is the ratio of oxygen to contaminant consumed.

BIOPLUME II has been applied for simulating dissolved-phase hydrocarbon transport and aerobic biodegradation (Chiang et al., 1989; Wiedemeier et al., 1994). BIOPLUME II accurately predicted the migration and attenuation of benzene, toluene, ethylbenzene, and xylene (BTEX) plume at Hill Air Force Base, Utah. The appropriateness and applicability of BIOPLUME II for

similar sites was evaluated and confirmed in the MADE-2 experiments (Beach et al., 1996). The MADE-2 project had controlled field experiments involving the injection of several aromatic hydrocarbons and a non-reactive tracer into an uncontaminated aquifer. Because of its instantaneous reaction assumption, BIOPLUME II is not usually used for simulating very slow aerobic biodegradation. BIOPLUME II does not simulate anaerobic processes affected by electron acceptors such as nitrate, ferric iron, sulfate, and inorganic carbon. However, BIOPLUME II has been popular because it is relatively easy to calibrate and apply using data such as hydrogeologic parameters, contaminant chemical and physical properties, contaminant source concentrations, and background oxygen concentration. We use BIOPLUME II to simulate aerobic biodegradation processes and contaminant transport within our S/O model. BIOPLUME III application to Site ST-29 at Patrick Air Force Base (Rifai et al., 2000) demonstrated natural attenuation suitability as a remedy for a fuel hydrocarbon plume. An intent of this article is to demonstrate a new optimization method and how it can employ a biodegradation simulator. The BIOPLUME model is assumed adequate for the purpose.

STUDY CASE

Figure 2 illustrates the hypothetical study area, initial contaminant plume, and candidate well locations considered by the optimization. Table 1 presents BIOPLUME II input parameters for the 510×690 m study area. The homogeneous aquifer has a hydraulic conductivity 6×10^{-5} m/s and 15 m aquifer thickness. To the west and east are fixed head boundaries: 30.5 and 27.7 m, respectively. Groundwater flow is from west to east. The initial hydraulic gradient is 0.004. To the north and south are no-flow boundaries. Groundwater flow simulation is steady state. The contaminant retardation factor is assumed to be 1. The organic contaminant resembles phenol in having high water solubility and a low soil sorption coefficient (Montgomery, 1996). Biodegradation occurs aerobically, and anaerobic decay is not considered. Figure 3 shows that if no action is taken, after 5 years the contamination has reached monitoring wells. Natural aerobic decay only reduces the total contaminant mass by 16%. An in-situ bioremediation system should be installed to contain the contaminant plume and enhance the biodegradation of contaminant.

To design an in-situ bioremediation system here, the optimization considers seven candidate injection wells and six candidate extraction wells. The S/O model will select from those while developing a least-cost design and pumping strategy. Injection wells within the plume can potentially inject oxygen and nutrient-laden water at rates between 0 and 1.26 L/s (20 gpm) per well. Upper and lower bounds of hydraulic head for the injection wells are 33.5 and 27.7 m, respectively. The initial oxygen concentration is 5 ppm except in the contaminant plume area. The background groundwater oxygen concentration is 5 ppm. Vertical oxygen exchange with the unsaturated zone is assumed to be insignificant. The injected oxygen concentration is 8 ppm. Downgradient wells can potentially extract contaminated groundwater at rates between 0 and 1.26 L/s (20 gpm). The upper and lower bounds of hydraulic head for the extraction wells are 30.5 and 24.4 m, respectively. The cleanup standard

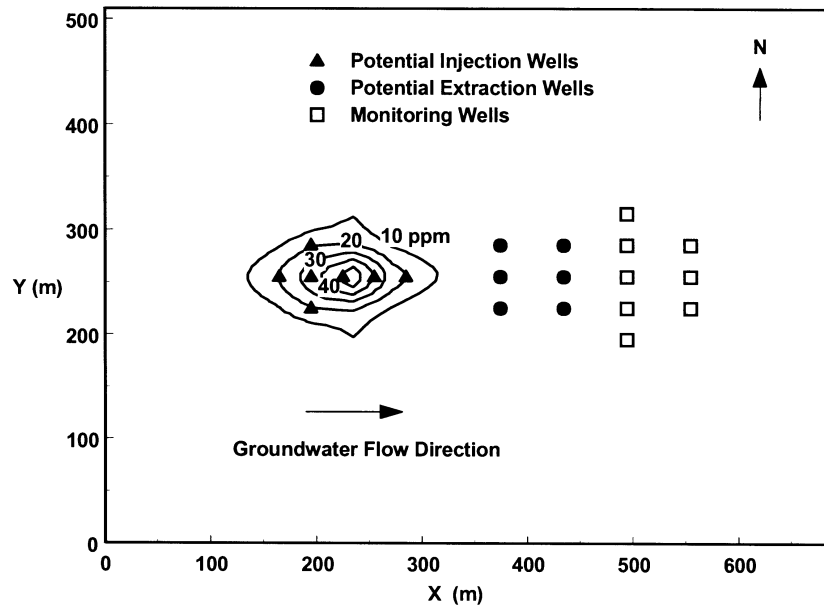


Figure 2. Proposed in-situ bioremediation system and initial contaminant plume.

Table 1. Input parameters of BIOPLUME II simulation model.

Input Parameter	Value
Grid size	19 × 25
Cell size	30 × 30 m
Hydraulic conductivity	6×10^{-5} m/s
Aquifer thickness	15 m
Hydraulic gradient	0.004
Longitudinal dispersivity	10 m
Transverse dispersivity	2 m
Effective porosity	0.3
Retardation factor	1.0
Anisotropy factor	1.0
Injected oxygen concentration	8 ppm
Background oxygen concentration	5 ppm
Remediation time	3 years

(C_{ci}) is 3 ppm for the entire study area. Eight monitoring wells are used to observe whether the plume is captured for a 3-year remediation period. The maximum contaminant concentration permitted to reach monitoring wells (C_{ca}) is 1 ppm.

Table 2 lists cost coefficients used to estimate system costs. The injection coefficient is based on the nutrients, oxygen, and pumping operation costs. The extraction coefficient considers the treatment and pumping cost for the contaminated groundwater. The treatment method combines air stripping and granular activated carbon. The capital cost of injection and treatment facilities is based on their capacities.

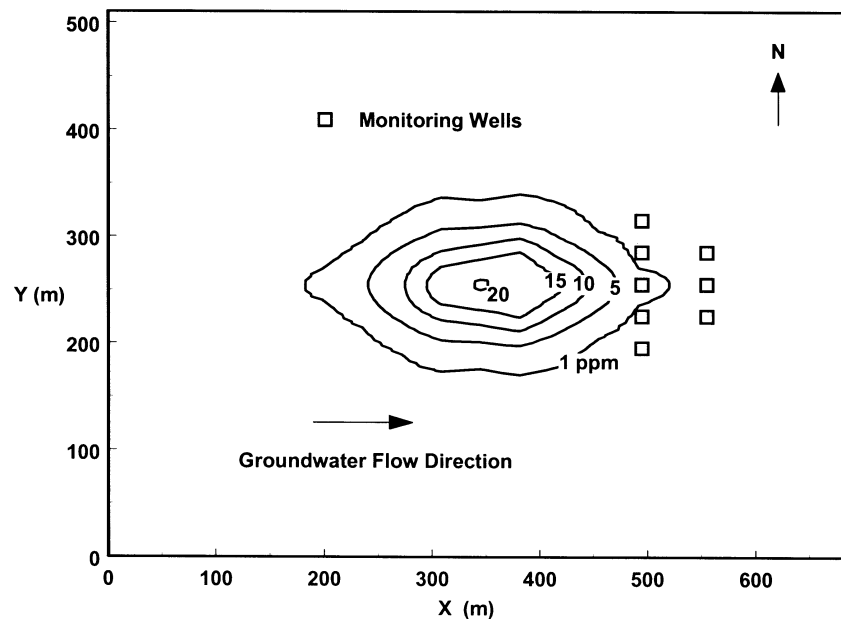


Figure 3. Unmanaged scenario: contaminant plume after 5 years of transport.

Table 2. Cost function coefficients.

Coefficient	Value
C ^P for injection cost (oxygen, nutrient, and pumping operation)	4,755 (\$ per L/s-year)
C ^P for extraction cost (treatment and pumping operation)	15,850 (\$ per L/s-year)
C ^{IP} (well installation cost)	12,000 (\$ per well)
D (injection facility capital cost)	D _{1.26 L/s (20 gpm)} = \$20,000 D _{2.52 L/s (40 gpm)} = \$24,000 D _{3.79 L/s (60 gpm)} = \$28,000 D _{5.05 L/s (80 gpm)} = \$32,000 D _{6.31 L/s (100 gpm)} = \$36,000 D _{7.57 L/s (120 gpm)} = \$40,000 D _{8.83 L/s (140 gpm)} = \$44,000
E (treatment facility capital cost)	E _{1.26 L/s (20 gpm)} = \$30,000 E _{2.52 L/s (40 gpm)} = \$38,000 E _{3.79 L/s (60 gpm)} = \$46,000 E _{5.05 L/s (80 gpm)} = \$54,000 E _{6.31 L/s (100 gpm)} = \$62,000 E _{7.57 L/s (120 gpm)} = \$70,000

Table 3. Optimal system cost comparison of four annealing schedules.

Temperature Update Functions	Initial Annealing Temp.	Final Annealing Temp.	Optimal System Cost (\$)	No. of Simulations
Equation 6 $\alpha = 0.99$	20,000	1000	241,400	9,495
Equation 6 $\alpha = 0.98$	20,000	1000	243,600	3,729
Equation 7	200,000	1000	280,900	3,109
Equation 8 $\delta = 0.06$	20,000	1000	244,000	4,505
Equation 9 $\lambda = 0.02$	20,000	1000	235,100	3,926

ANALYSIS OF ANNEALING SCHEDULES

The most important CSA component is the annealing schedule (AS), which controls convergence to optimal solutions. This is the first article to compare the performance

of ASs for SA application to groundwater management problems. We contrast four ASs that differ primarily in the employed TUF, but one AS also uses a different initial temperature. Utilized are two static TUFs (eqs. 6 and 7) and two adaptive TUFs (eqs. 8 and 9). Employed AS parameters (table 3) were selected based on preliminary simulations, to balance between desirable convergence and computational cost (table 3). The AS using TUF equation 7 employs an initially high 200,000 annealing temperature to permit a fast temperature decrease. The number of movements in the inner loop is 130. This numerical experiment employs Corana’s NF to generate new system configurations, and while annealing temperature is decreasing, system configuration changes are controlled by threshold accepting function.

For the four TUFs, table 3 shows the minimum system costs and the numbers of simulations required to achieve those costs. Adaptive TUF equation 9 required 3,926 simulations to obtain the lowest cost of all. The design produced by TUF equation 6 with $\alpha = 0.98$ was slightly more costly, but required fewer simulations. Model simulations usually consume 99% of computational cost in this S/O model. The fewer simulations, the less computation time.

Figure 4 shows how total bioremediation system cost evolves with decreasing CSA temperature. Optimal system cost is achieved after annealing temperature drops below 1,000. The static AS of equation 7 has the fastest temperature decrease, and uses the fewest simulations, but freezes its optimal solution prematurely, yielding the highest system design cost: \$280,900. Equation 9 yields the lowest system costs of \$235,100. Figure 5 shows system cost improvement with increasing number of BIOPLUME II simulations. Equations 6, 8, and 9 yield similar system costs (\$244,000 to \$235,100), but equation 6 with $\alpha = 0.98$ requires the least number of BIOPLUME II model simulations. Because of its satisfactory CPU computational requirement, and optimal solution quality, the annealing schedule of equation 6 with $\alpha = 0.98$ was chosen for use in ten different in-situ bioremediation design scenarios in the next section.

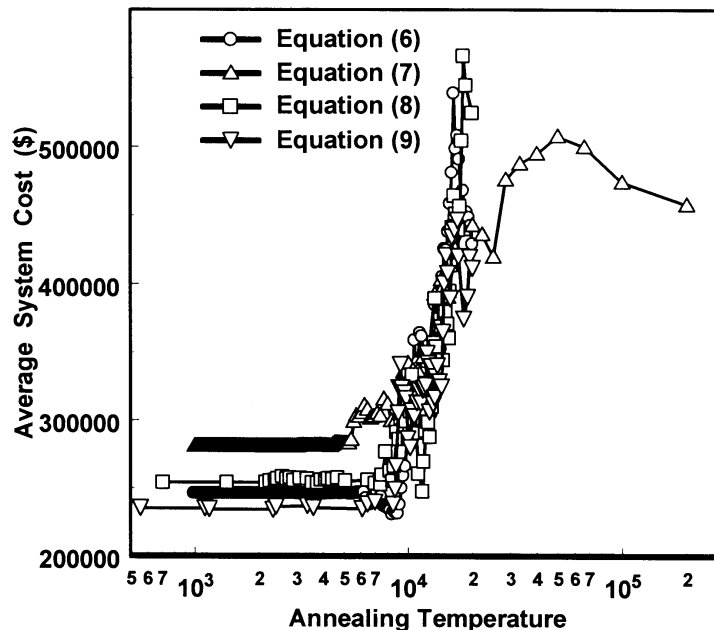


Figure 4. Comparison of average system cost vs. annealing temperature using four temperature update functions (eq. 6 with $\alpha = 0.98$).

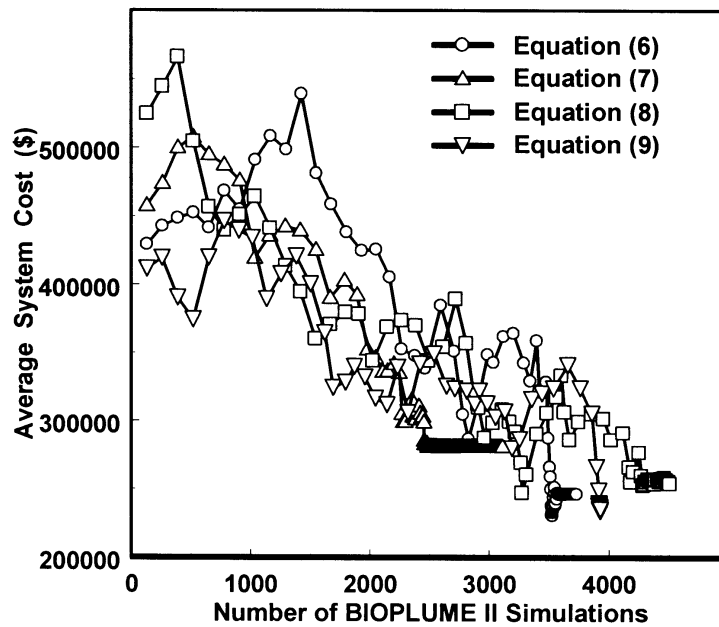


Figure 5. Comparison of average system cost vs. number of BIOPLUME II simulations using four temperature update functions (eq. 6 with $\alpha = 0.98$).

OPTIMAL IN-SITU BIOREMEDIATION SYSTEM DESIGN FOR TEN SCENARIOS

Ten scenarios demonstrate how computed optimal bioremediation strategies differ depending on assumed injected oxygen concentration, hydraulic conductivity, longitudinal dispersivity, retardation factor, and remediation time. Table 4 shows assumptions and results. All optimal results are obtained by CSA using AS equation 6 and Corana's NF.

Scenario 1: Base Case

The base scenario is the same as in the previous section for comparing the performance of the four ASs. The annealing schedule of equation 6 with $\alpha = 0.98$ is applied in the CSA for the optimal system design of the base scenario. Table 1 shows BIOPLUME II input parameters. This base case optimal system design requires four injection wells and three extraction wells (fig. 6). The maximum contaminant concentration is reduced to 3 ppm, and no contamination reaches the monitoring wells. Approximately 90% of the initial contaminant mass is eliminated. Injection and extraction totaled 2.65 L/s (42.0 gpm) and 1.14 L/s (18.1 gpm), respectively. Figure 7 illustrates the resulting steady-state hydraulic head distribution. The injection

wells recharged nutrients and oxygen to stimulate contaminant biodegradation, but also caused localized hydraulic head rise and induced contaminant spread. Extraction wells created gradient barriers, preventing downstream contaminant plume migration, and extracted contaminants for further in-situ treatment. The total system cost is \$234,000, including extraction, injection, and treatment, and facilities capital costs.

Scenario 2: Effects of High Injected Oxygen Concentration on System Design

In this scenario, we increase oxygen delivery by employing pure oxygen (40 mg/L oxygen concentration) at a cost of \$17,435 per L/s-year (\$1,100 per gpm-year). Although hydrogen peroxide (H_2O_2) can provide a higher oxygen concentration, it is not used here because it is toxic to some microorganisms at concentrations of 100 to 200 mg/L³, and delivery is inefficient (Ritter and Scarborough, 1995; Alexander, 1999). The result is less injection but more extraction and total cost. The high oxygen concentration reduces the injection rate. The total system cost is \$278,200, which is higher than the base scenario 1 because of increasing extraction wells installation and operation costs.

Table 4. Optimal system design of in-situ bioremediation for ten scenarios.

Scenario	No. of Injection Wells	No. of Extraction Wells	Total Injection Rate (L/s)	Total Extraction Rate (L/s)	Total System Cost (\$)
1: Base case ^[a]	4	3	2.65	1.14	234,000
2: Injected oxygen concentration = 40 mg/L	4	4	0.97	1.55	278,200
3: Hydraulic conductivity = 1×10^{-4} m/s	5	3	2.17	1.17	236,400
4: Hydraulic conductivity = 1×10^{-5} m/s	6	3	3.46	1.70	304,300
5: Longitudinal dispersivity = 3 m	5	2	2.13	1.89	265,900
6: Longitudinal dispersivity = 30 m	6	0	3.27	0.0	146,700
7: Retardation factor = 1.5	7	2	5.51	0.28	265,800
8: Retardation factor = 2.0	6	2	10.24	0.14	330,600
9: Remediation time = 2 years	6	3	3.90	2.13	282,500
10: Remediation time = 4 years	7	0	5.32	0.0	221,300

^[a] Base case: injected oxygen concentration = 8 ppm, hydraulic conductivity = 6×10^{-5} m/s, longitudinal dispersivity = 10 m, retardation factor = 1.0, and remediation time = 3 years.

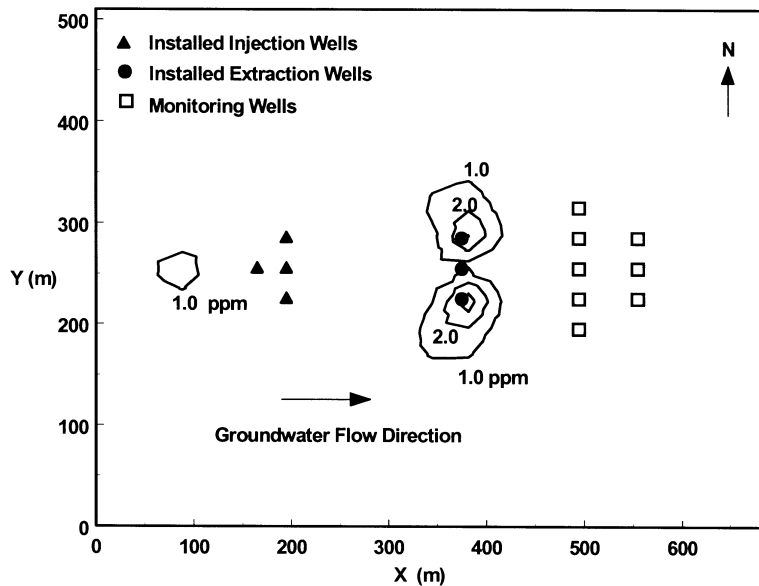


Figure 6. Contaminant plume of base scenario after 3 years of in-situ bioremediation.

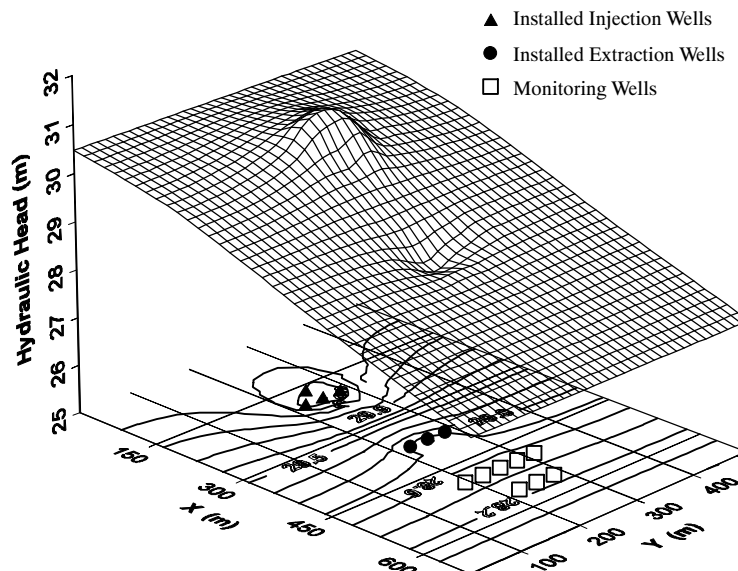


Figure 7. Hydraulic head distribution of base scenario after 3 years of in-situ bioremediation.

Scenarios 3 and 4: Effects of Hydraulic Conductivity on System Design

The more homogeneous and isotropic the aquifer, the better for successful in-situ bioremediation (Rittmann et al., 1994). Ideal hydraulic conductivity should range from 10^{-6} to 10^{-4} m/s or greater (Rittmann et al., 1994; Norris et al., 1996). Table 4 shows that increasing hydraulic conductivity reduces total pumping and system cost, and decreasing hydraulic conductivity increases cost. The higher the hydraulic conductivity, the more efficient the oxygen delivery.

Scenarios 5 and 6: Effects of Longitudinal Dispersivity on System Design

Mass transport by advection and dispersion affects contaminant distribution and substrate/electron acceptor availability to microorganisms (Sturman et al., 1995). Scenarios 5 and 6 employ longitudinal dispersivities of 3 m and 30 m, respectively, which are in the reliable range of field-scale data described by (Gelhar et al., 1992). Reducing longitudinal dispersivity caused increased system cost. Increasing longitudinal dispersivity permits reduced cost. The optimal design for the 30 m dispersivity only requires injection wells and facility, and costs only \$146,700, i.e., 45% less than the system designed for the longitudinal dispersivity of 3 m (table 4). Figure 8 compares final oxygen concentration distributions for the two scenarios and optimal designs. The greater the longitudinal dispersivity, the greater

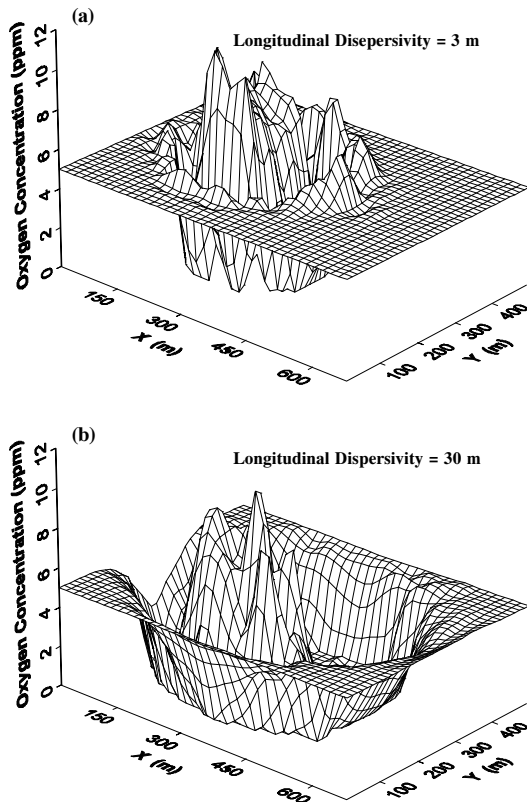


Figure 8. Oxygen concentration distribution after 3 years of in-situ bioremediation: (a) longitudinal dispersivity = 3 m, and (b) longitudinal dispersivity = 30 m.

the oxygen mixing with contaminants and the greater the biodegradation.

Scenarios 7 and 8: Effects of Retardation Factor on System Design

In groundwater modeling, sorption is approximated by retarding contaminant movement relative to the groundwater. A retardation factor is modeled as a function of partition coefficient, soil bulk density, and porosity. A retardation factor of 2 implies that the contaminant moves at half the groundwater velocity. Most retardation models assume linear adsorption isotherms between solute and solid phase concentrations. This is usually true only in homogeneous aquifers. The base scenario retardation factor of 1 permits the contaminant to have the same velocity as the groundwater. In scenarios 7 and 8, as retardation factor increases, extraction decreases, but injection and total cost increase. Extraction wells cannot easily remove adsorbed contaminant, sometimes causing cleanup failure.

Scenarios 9 and 10: Effects of Remediation Time on System Design

Remediation period duration is often determined by budgetary constraint, priority, and legal deadlines. Table 4 illustrates the effect on strategy design of remediation time: 2 years (scenario 9), 3 years (scenario 1), and 4 years (scenario 10). The shorter the remediation period, the higher the total system cost. The short 2-year remediation requires large injection and extraction rates to enhance biodegradation. The optimal system design for a 4-year remediation period does not require extraction, but employs a high 5.32 L/s (84.4 gpm) oxygen injection rate. The longer

remediation period provides time for slow oxygen mixing and transport.

CONCLUSION

The presented continuous simulated annealing-BIOPLUME II model optimizes in-situ bioremediation system design. This new S/O model determines the pumping (extraction/injection) strategy that minimizes total system cost, reduces contaminant concentration to cleanup standard, and prevents contaminant plume migration. It is the first bioremediation S/O model to use a continuous simulated annealing for optimal system design. Here the pumping rates are treated as continuous variables by implementing neighborhood functions to generate new system configurations. Corana's neighborhood function effectively searches the continuous solution space. Contrasting optimal designs developed by four simulated annealing temperature update functions (TUFs) showed that an adaptive TUF developed the best strategy. However, a geometric TUF provided nearly as good a strategy, and a good compromise between solution optimality and computational effort.

Site properties significantly affect optimal in-situ bioremediation system design. Bioremediation improves with increasing hydraulic conductivity, longitudinal dispersivity, and remediation period and with decreasing retardation factor. Increasing longitudinal dispersivity aids bioremediation and reduces system cost by 45%. Increasing retardation factor requires greater injection rates and increases system costs. Increasing injected oxygen concentration reduces necessary injection rate but increases total system cost by increasing well installation and extraction costs.

The presented CSA and CSA-based S/O model are valuable tools for designing in-situ bioremediation system. CSA can readily consider all installation, operation, and maintenance costs to yield optimal site-specific system designs. Such a design includes optimal well locations, pumping rates, and facility capacities.

ACKNOWLEDGEMENTS

This article was supported by the Utah Agricultural Experiment Station, Utah State University, Logan, Utah (approved as Journal Paper No. 7744) and by Diwan University, Tainan, Taiwan (Project No. DWU95C24).

REFERENCES

- Aarts, E., and J. Korst. 1989. *Simulated Annealing and Boltzmann Machines*. New York, N.Y.: John Wiley.
- Aarts, E. H., and P. J. M. van Laarhoven. 1985. Statistical cooling: A general approach to combinatorial optimization problems. *Philips J. Res.* 40(4): 193-226.
- Alexander, M. 1999. *Biodegradation and Bioremediation*. San Diego, Cal.: Academic Press.
- Althofer, I., and K.-U. Koschnick. 1991. On the convergence of "threshold accepting". *Appl. Math. Optimization* 24: 183-195.
- Aly, A. H., and R. C. Peralta. 1999. Comparison of a genetic algorithm and mathematical programming to the design of groundwater cleanup system. *Water Resour. Res.* 35(8): 2415-2426.
- Beach, J., D. Fryar, H. Rifai, K. Appling, and T. B. Stauffer. 1996. Evaluation of natural attenuation of organic tracers at the MADE

- site using the Bioplume II transport model. Technical report. Austin, Tex.: INTERA, Inc.
- Bennage, W. A., and A. K. Dhingra. 1995. Single and multiobjective structural optimization in discrete-continuous variables using simulated annealing. *Intl. J. Numerical Methods in Eng.* 38(16): 2753-2773.
- Bohachevsky, I. O., M. E. Johnson, and M. L. Stein. 1986. Generalized simulated annealing for function optimization. *Technometrics* 28(3): 209-217.
- Borden, R. C., and P. B. Bedient. 1986. Transport of dissolved hydrocarbons influenced by oxygen-limited biodegradation: 1. Theoretical development. *Water Resour. Res.* 22(13): 1973-82.
- Cerny, V. 1985. Thermodynamical approach to the traveling salesman problem: An efficient simulation algorithm. *J. Optim. Theory Appl.* 45(1): 41-51.
- Chan Hilton, A. B., and T. B. Culver. 2005. Groundwater remediation design under uncertainty using genetic algorithms. *J. Water Resour. Plan. Mgmt.* 131(1): 25-34.
- Chiang, C. Y., J. P. Salanitro, E. Y. Chai, J. D. Colthart, and C. L. Klein. 1989. Aerobic biodegradation of benzene, toluene, and xylene in a sandy aquifer: Data analysis and computer modeling. *Ground Water* 27(6): 823-834.
- Cookson, J. T. 1995. *Bioremediation Engineering: Design and Application*. New York, N.Y.: McGraw-Hill.
- Cooper, G. S., R. C. Peralta, and J. J. Kaluarachchi. 1998. Optimizing separate phase light hydrocarbon recovery from contaminated unconfined aquifers. *Adv. Water Resour.* 21(5): 339-350.
- Corana, A., M. Marchesi, C. Martini, and S. Ridella. 1987. Minimizing multimodal functions of continuous variables with the simulated annealing algorithm. *ACM Trans. Math. Software* 13(3): 262-280.
- Culver, T. B., and C. A. Shoemaker. 1997. Dynamic optimal ground-water reclamation with treatment capital cost. *J. Water Resour. Plan. Mgmt.* 123(1): 23-29.
- Dekkers, A., and E. Aarts. 1991. Global optimization and simulated annealing. *Math. Programming* 50: 367-393.
- Dougherty, D. E., and R. A. Marryott. 1991. Optimal groundwater management: 1. Simulated annealing. *Water Resour. Res.* 27(10): 2493-2508.
- Dueck, G., and T. Scheuer. 1990. Threshold accepting: A general purpose optimization algorithm appearing superior to simulated annealing. *J. Comput. Physics* 90: 161-175.
- Espinoza, F. P., B. S. Minsker, and D. E. Goldberg. 2005. Adaptive hybrid genetic algorithm for groundwater remediation design. *J. Water Resour. Plan. Mgmt.* 131(1): 14-24.
- Essaid, H. I., B. A. Bekins, E. M. Godsy, E. Warren, M. J. Baedeker, and I. M. Cozzarelli. 1995. Simulation of aerobic and anaerobic biodegradation processes at a crude oil spill site. *Water Resour. Res.* 31(12): 3309-3327.
- Gelhar, L. W., C. Welty, and K. R. Rehfeldt. 1992. A critical review of data on field-scale dispersion in aquifers. *Water Resour. Res.* 28(7): 1955-1974.
- Geman, S., and D. Geman. 1984. Stochastic relaxation, Gibbs distributions, and the Bayesian restoration of images. *IEEE Trans. Pattern Anal. and Mach. Intell.* 6(6): 721-741.
- Gopalakrishnan, G., B. S. Minsker, and D. E. Goldberg. 2003. Optimal sampling in a noisy genetic algorithm for risk-based remediation design. *J. Hydroinformatics* 5(1): 11-25.
- Hajek, B. 1988. Cooling schedules for optimal annealing. *Math. Oper. Res.* 13(2): 311-329.
- Huang, M. D., F. Romeo, and A. Sangiovanni-Vincentelli. 1986. An efficient general cooling schedule for simulated annealing. In *Proc. 1986 IEEE Intl. Conf. on Computer-Aided Design*, 381-384. Washington, D.C.: IEEE Computer Society Press.
- Ingber, L. 1989. Very fast simulated re-annealing. *Math. Comput. Modelling* 12(8): 967-973.
- Johnson, V. M., and L. L. Rogers. 2000. Accuracy of neural network approximators in simulation-optimization. *J. Water Resour. Plan. Manage.* 126(2): 48-56.
- Joines, J. A., and C. R. Houck. 1994. On the use of the non-stationary penalty functions to solve nonlinear constrained optimization problems with GA's. In *Proc. 1st IEEE Conference on Evolutionary Computation*, 579-584. Piscataway, N.J.: IEEE.
- Kalwij, I., and R. Peralta. 2006. Simulation/optimization modeling for robust pumping strategy design. *Ground Water* 44(4): 574-582.
- Kirkpatrick, S., C. D. Gelatt, and M. P. Vecchi. 1983. Optimization by simulated annealing. *Science* 220(4598): 671-680.
- Konikow, L. F., and J. D. Bredehoeft. 1978. *Computer Model of Two-Dimensional Solute Transport and Dispersion in Ground Water*. Washington, D.C.: Techniques of Water Resources Investigation of the USGS.
- Kuo, C.-H., A. N. Michel, and W. G. Gray. 1992. Design of optimal pump-and-treat strategies for contaminated groundwater remediation using the simulated annealing algorithm. *Adv. Water Resour.* 15(2): 95-105.
- Lin, C. K. Y., K. B. Haley, and C. Sparks. 1995. A comparative study of both standard and adaptive versions of threshold accepting and simulated annealing algorithms in three scheduling problems. *European J. Oper. Res.* 83(2): 330-346.
- MacQuarrie, K. T. B., E. A. Sudicky, and E. O. Frind. 1990. Simulation of biodegradable organic contaminants in groundwater: 1. Numerical formulation of principal directions. *Water Resour. Res.* 26(2): 207-222.
- Malone, D. R., C. M. Kao, and R. C. Borden. 1993. Dissolution and bioremediation of nonaqueous phase hydrocarbons: Model development and laboratory evaluation. *Water Resour. Res.* 29(7): 2203-2213.
- Marryott, R. A. 1996. Optimal ground-water remediation design using multiple control technologies. *Ground Water* 34(3): 425-433.
- Marryott, R. A., D. E. Dougherty, and R. L. Stollar. 1993. Optimal groundwater management: 2. Application of simulated annealing to a field-scale contamination site. *Water Resour. Res.* 29(4): 847-860.
- McKinney, D. C., and M.-D. Lin. 1994. Genetic algorithm solution of groundwater management models. *Water Resour. Res.* 30(6): 1897-1906.
- Metropolis, N., A. W. Rosenbluth, M. N. Rosenbluth, A. H. Teller, and E. Teller. 1953. Equation of state calculations by fast computing machines. *J. Chem. Physics* 21(6): 1087-1092.
- Michalewicz, Z., and N. F. Attia. 1994. Evolutionary optimization of constrained problems. In *Proc. 3rd Annual Conference on Evolutionary Programming*, 98-108. A. V. Sebald and J. Fogel, eds. River Edge, N.J.: World Scientific Publishing.
- Minsker, B. S., and C. A. Shoemaker. 1996. Differentiating a finite element biodegradation simulation model for optimal control. *Water Resour. Res.* 32(1): 187-192.
- Minsker, B. S., and C. A. Shoemaker. 1998. Dynamic optimal control of in situ bioremediation of ground water. *J. Water Resour. Plan. Mgmt.* 124(3): 149-161.
- Montgomery, J. H. 1996. *Groundwater Chemicals Desk Reference*. Boca Raton, Fla.: Lewis Publishers.
- Moscato, P., and J. F. Fontanari. 1990. Stochastic versus deterministic update in simulated annealing. *Physics Letters A* 146(4): 204-208.
- Norris, R. D., R. E. Hinchee, R. Brown, P. L. McCarty, L. Semprini, J. T. Wilson, D. H. Campbell, M. Reinhard, E. J. Bouwer, R. C. Borden, T. M. Vogel, J. M. Thomas, and C. H. Ward. 1996. *Handbook of Bioremediation*. Boca Raton, Fla.: Lewis Publishers.

- Otten, R. H. J. M., and L. P. P. van Ginneken. 1989. *The Annealing Algorithm*. Boston, Mass.: Kluwer Academic Publishers.
- Peralta, R. C., I. Kalwij, and S. Wu. 2008. Practical remedial design optimization for large complex plumes. *J. Water Resour. Plan. Mgmt.* 134(5): (in press).
- Reed, P., B. S. Minsker, and D. E. Goldberg. 2000. Designing a competent simple genetic algorithm for search and optimization. *Water Resour. Res.* 36(12): 3757-3762.
- Ren, X., and B. S. Minsker. 2005. Which groundwater remediation objective is better: A realistic one or a simple one? *J. Water Resour. Plan. Mgmt.* 131(5): 351-361.
- Rifai, H. S., and P. B. Bedient. 1990. Comparison of biodegradation kinetics with an instantaneous reaction model for groundwater. *Water Resour. Res.* 26(4): 637-645.
- Rifai, H. S., P. B. Bedient, J. T. Wilson, K. M. Miller, and J. M. Armstrong. 1988. Biodegradation modeling at aviation fuel spill site. *J. Environ. Eng.* 114(5): 1007-1029.
- Rifai, H. S., C. J. Newell, J. R. Gonzales, and J. T. Wilson. 2000. Modeling natural attenuation of fuels with BIOPLUME III. *J. Environ. Eng.* 126(5): 428-438.
- Ritter, W. F., and R. W. Scarborough. 1995. A review of bioremediation of contaminated soils and groundwater. *J. Environ. Sci. Health A30(2)*: 333-357.
- Rittmann, B. E., E. Seagren, B. A. Wrenn, A. J. Valocchi, C. Ray, and L. Raskin. 1994. *In Situ Bioremediation*. Park Ridge, N.J.: Noyes Publications.
- Rizzo, D. M., and D. E. Dougherty. 1996. Design optimization for multiple management period groundwater remediation. *Water Resour. Res.* 32(8): 2549-2561.
- Rogers, L. L., and F. U. Dowla. 1994. Optimization of groundwater remediation using artificial neural networks with parallel solute transport modeling. *Water Resour. Res.* 30(2): 457-81.
- Romeo, F., and A. Sangiovanni-Vincentelli. 1985. Probabilistic hill climbing algorithms: Properties and applications. In *Proc. 1985 Chapel Hill Conference Very Large Scale Integration*, 393-417. H. Fuchs, ed. Rockville, Md.: Computer Science Press.
- Romeo, F., and A. Sangiovanni-Vincentelli. 1991. A theoretical framework for simulated annealing. *Algorithmica* 6: 302-345.
- Smalley, J. B., B. S. Minsker, and D. E. Goldberg. 2000. Risk-based in situ bioremediation design using a noisy genetic algorithm. *Water Resour. Res.* 36(10): 3043-3052.
- Stiles, G. S. 1994. The effect of numerical precision upon simulated annealing. *Physics Letters A* 185: 253-261.
- Sturman, P. J., P. S. Stewart, A. B. Cunningham, E. J. Bouwer, and J. H. Wolfram. 1995. Engineering scale-up of in situ bioremediation process: A review. *J. Contam. Hydrol.* 19(2): 171-203.
- Sun, Y.-H., M. W. Davert, and W. Y.-G. Yeh. 1996. Soil vapor extraction system design by combinatorial optimization. *Water Resour. Res.* 32(6): 1863-1873.
- Szu, H., and R. Hartley. 1987. Fast simulated annealing. *Physics Letters A* 122(3-4): 157-162.
- Vanderbilt, D., and S. G. Louie. 1984. A Monte Carlo simulated annealing approach to optimization over continuous variable. *J. Comput. Physics* 56(2): 259-271.
- van Laarhoven, P. J. M., and E. H. L. Aarts. 1987. *Simulated Annealing: Theory and Applications*. Dordrecht, The Netherlands: D. Reidel Publishing.
- Wang, M., and C. Zheng. 1998. Ground water management optimization using genetic algorithms and simulated annealing. *J. American Water Resour. Assoc.* 34(3): 519-530.
- Wang, P. P., and D.-S. Chen. 1996. Continuous optimization by a variant of simulated annealing. *Computational Optimization and Applications* 6(1): 59-71.
- Wiedemeier, T. H., J. T. Wilson, R. N. Miller, and D. H. Kampbell. 1994. United States Air Force guidelines for successfully supporting intrinsic remediation with an example from Hill Air Force Base. In *Proc. Petroleum Hydrocarbons and Organic Chemicals in Ground Water: Prevention, Detection, and Restoration*, 317-334. Houston, Tex.: National Ground Water Association and American Petroleum Institute.
- Yoon, J.-H., and C. A. Shoemaker. 1999. Comparison of optimization methods for ground-water bioremediation. *J. Water Resour. Plan. Mgmt.* 125(1): 54-63.
- Yoon, J.-H., and C. A. Shoemaker. 2001. Improved real-coded GA for groundwater bioremediation. *J. Computing in Civil Eng.* 15(3): 224-231.

